the $\ln s/s$ term which gives the dominant behavior at large s, one sees that the box amplitude provides a concrete example of a situation where a contribution of type (b) is important at high energy. In other words, if only the on-shell contribution had been retained one would have obtained an incorrect high-energy form for the box amplitude.

To check that the first term in (10) gives the correct leading term, the t_1 and t_3 integrations can be done to give

$$\phi(t)=\frac{2\pi}{[t(t-4\mu^2)]^{1/2}}\ln\left(\frac{-t+[t(t-4\mu^2)]^{1/2}}{t+[t(t-4\mu^2)]^{1/2}}\right), \quad (14)$$

and therefore

$$A(s,t)=\frac{g^4}{8\pi^2}\frac{1}{[t(t-4\mu^2)]^{1/2}}\ln\left(\frac{-t+[t(t-4\mu^2)]^{1/2}}{t+[t(t-4\mu^2)]^{1/2}}\right)\frac{\ln s}{s}+\cdots, \quad (15)$$

which is the same as (2).

In conclusion we feel that this example suggests that the off-shell contribution to iterated scattering amplitudes is important at high energy (if one believes field theory). Consequently, any iterative scheme which does not include this contribution may make a serious omission. Since the absorption and eikonal formalisms apparently do just this, their ability to generate believable corrections to Regge-pole exchanges is questionable.

PHYSICAL REVIEW VOLUME 177, NUMBER 5 25 JANUARY 1969

ρ Bootstrap in the Unitarized Strip Approximation

P. D. B. COLLINS AND R. C. JOHNSON*
Physics Department, University of Durham, Durham City, England
(Received 15 July 1968)

We present a method of improving the new strip approximation of Chew and Jones by calculating parts of the elastic double spectral functions using the Mandelstam iteration procedure. These double spectral functions are used to obtain additional contributions to the left-hand cuts of the partial-wave amplitudes, and also to estimate the inelasticity within the strip region. The inelastic N/D equations are solved in the way proposed by Frye and Warnock. The method is applied to the problem of bootstrapping the ρ trajectory in π-π scattering, and some preliminary results are presented. We find that it is possible to obtain a self-consistent trajectory with the correct physical mass, width, and intercept $\alpha(0)$, but that the solution is by no means unique, since self-consistency can be achieved with trajectories having intercepts anywhere from $\alpha(0)=1$ to $\alpha(0)\approx 0.2$. Also, the trajectories have a large curvature, and large residue, which result in a violation of crossed-channel unitarity for low l.

I. INTRODUCTION

OVER the past few years many attempts have been made to demonstrate that the ρ meson approximately "bootstraps" itself in π-π scattering.[1–10] The zero external spins and equal-mass kinematics make this one of the most attractive bootstrap problems, but as more sophisticated methods have been applied to the problem, it has become clear that while many qualitative features support the bootstrap hypothesis, the quantitative details of the solutions to the various models are very unsatisfactory.[8,10]

Probably the most comprehensive approach has been the so-called "new form" of the strip approximation devised by Chew and Jones,[11,12] which parametrizes the amplitude in terms of the Regge poles in each channel, and then uses the N/D equations to impose unitarity and so determine the Regge parameters. However, it has been found that this approximation is inadequate,[10] one of its principal deficiencies being that it includes the forces only in the first Born approximation. It has been shown recently that the N/D equations for nonrelativistic potential scattering give much more satisfactory results if the forces are included up to at least the third Born approximation,[13] and we can expect that this will also be true in relativistic calculations.

* R. C. Research Student; present address: Physics Department, Toronto University, Toronto 5, Canada.

[1] A fairly complete account of the background to this work can be found in P. D. B. Collins and E. J. Squires, *Regge Poles in Particle Physics* (Julius Springer-Verlag, Berlin, 1968).
[2] F. Zachariasen, Phys. Rev. Letters **7**, 112 (1961); **7**, 268(E) (1961).
[3] L. A. P. Balázs, Phys. Rev. **128**, 1939 (1962); **129**, 872 (1963).
[4] F. Zachariasen and C. Zemach, Phys. Rev. **128**, 849 (1962).
[5] J. Fulco, G. L. Shaw, and D. Wong, Phys. Rev. **137**, B1242 (1965).
[6] B. H. Bransden, P. G. Burke, J. W. Moffat, R. G. Moorhouse, and D. Morgan, Nuovo Cimento **30**, 207 (1963).
[7] N. F. Bali, G. F. Chew, and S.-Y. Chiu, Phys. Rev. **150**, 1352 (1966).
[8] N. F. Bali, Phys. Rev. **150**, 1358 (1966).
[9] P. D. B. Collins and V. L. Teplitz, Phys. Rev. **140**, B663 (1965).
[10] P. D. B. Collins, Phys. Rev. **142**, 1163 (1966). We follow the notation, etc., of this paper.
[11] G. F. Chew, Phys. Rev. **129**, 2363 (1963).
[12] G. F. Chew and C. E. Jones, Phys. Rev. **135**, B208 (1964).
[13] P. D. B. Collins and R. C. Johnson, Phys. Rev. **169**, 1222 (1968).

Higher Born approximations, for the region of energies where two-particle unitarity holds, can be calculated using the Mandelstam iteration method.[14] This formed the basis of the old strip approximation,[15] and has been revived recently for the ρ bootstrap by Bali *et al.*[7] These authors made a large number of iterations of the potential given by fixed-spin particle exchange until they could identify the crossed-channel asymptotic behavior, and used this behavior to obtain the Regge parameters (see Sec. II). The disadvantages of the iterative method are that very high numerical accuracy is needed to obtain the Regge parameters, and that it is not easy to improve the calculations by including inelastic effects, etc. By comparison the N/D equations enable one to obtain accurate Regge parameters with comparatively simple calculations, and to include inelasticity in a fairly straightforward way.

Our intention in this paper is to try and combine the advantages of both methods, by continuing to use the N/D equations with the potential calculated in the new strip approximation, but using the Mandelstam method to calculate parts of the double spectral functions, and hence higher Born approximations to the left-hand cut. At the same time we obtain information about the inelasticity within the strip region, and can use this as part of the input for the N/D equations, which are solved in the form suggested by Frye and Warnock.[16]

The basic assumptions of the approximation are of course the same as those of the new strip approximation.[12] We suppose that the π-π scattering amplitude can be divided into a high-energy region controlled by the leading Regge poles in the crossed channel, together with a low-energy region containing the direct-channel poles. In the low-energy region the dynamics are supposed to be mainly in the elastic channel, the modifications produced by the inelastic channels being small, though not negligible. In particular we do not consider the possibility that the low-energy resonances may be Castillejo-Dalitz-Dyson (CDD) poles in the channels we are looking at, despite recent evidence that this may be the case.[17,18] Thus what we are presenting is really just a better approximation to the equations implied by the strip approximation, and there is no change in the basic assumptions as they were explained in Ref. 12.

In the Secs. II–IV we present the details of the bootstrap scheme we are proposing. Although this scheme may obviously be applied to many types of bootstrap problem, here we have restricted ourselves to a discussion of π-π scattering and have incorporated zero spin, equal-mass kinematics, and the π-π isotopic-spin crossing matrix from the start. In Secs. V and VI we describe the results of an attempt to bootstrap the ρ trajectory in the π-π scattering amplitude. This is not our final answer to this problem because the effect of $I=0$ exchanges (the Pomeranchon, etc.) is neglected. It is well known[10,19] that the exchange of this trajectory presents special problems which we hope to cover in a later publication. Also there is the advantage that the inclusion of only one trajectory enables us to make a comprehensive search for self-consistent solutions, and to examine thoroughly the effect of the cut-off parameters on our results.

Some conclusions are presented in Sec. VII.

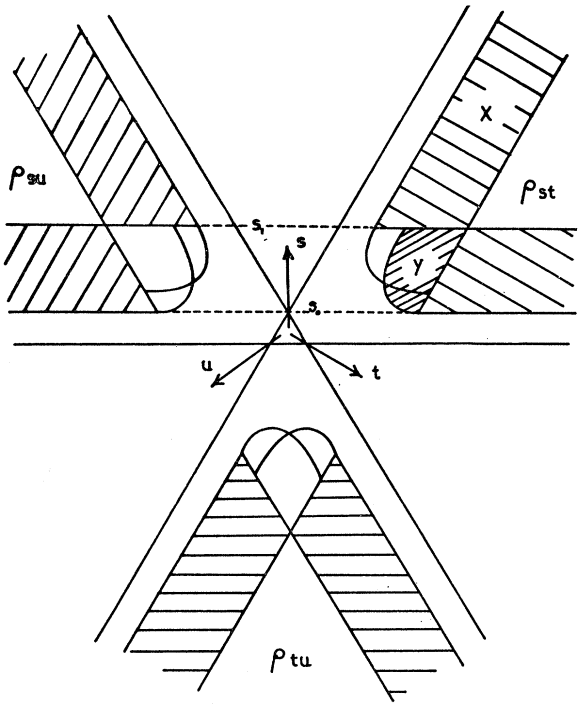

FIG. 1. The Mandelstam diagram showing the strips (shaded), and the curved boundaries of the elastic double spectral functions. The elastic s-channel double spectral function is marked Y. s_0 is the threshold, and s_1 the strip width, in the s channel.

II. CALCULATION OF THE POTENTIAL

The new form of the strip approximation, introduced by Chew and Jones,[12] consists of representing the two-particle scattering amplitude by strips of double spectral function adjacent to the physical regions, as shown in Fig. 1. The amplitude is assumed to satisfy the Mandelstam representation, which, in terms of the

[14] S. Mandelstam, Phys. Rev. **112**, 1344 (1958).
[15] G. F. Chew and S. C. Frautschi, Phys. Rev. **123**, 1478 (1961).
[16] G. Frye and R. L. Warnock, Phys. Rev. **130**, 478 (1963).
[17] P. D. B. Collins, R. C. Johnson, and E. J. Squires, Phys. Letters **26B**, 223 (1968).
[18] S. Mandelstam, in *1966 Tokyo Summer Lectures in Theoretical Physics*, edited by G. Takeda and A. Fuji (W. A. Benjamin, Inc., New York, 1966), Part II; and Phys. Rev. **166**, 1539 (1968).
[19] G. F. Chew, Phys. Rev. **140**, B1427 (1965).

usual invariants, may be written[1]

$$A(s,t)=\frac{1}{\pi}\int_{t_0}^{\infty}\frac{D_t(s,t')}{t'-t}dt'+\frac{1}{\pi}\int_{u_0}^{\infty}\frac{D_u(s,u')}{u'-u}du'$$
$$=\frac{1}{\pi^2}\int^{\infty}\int\frac{\rho_{st}(s'',t')}{(s''-s)(t'-t)}ds''dt'$$
$$+\frac{1}{\pi^2}\int^{\infty}\int\frac{\rho_{su}(s'',u')}{(s''-s)(u'-u)}ds''du'$$
$$+\frac{1}{\pi^2}\int^{\infty}\int\frac{\rho_{tu}(t',u'')}{(t'-t)(u''-u)}dt'du'', \quad (2.1)$$

the D's being the discontinuities and the ρ's the double spectral functions. Here t_0 and u_0 are the thresholds in the t and u channels, respectively. However, we shall always be concerned with amplitudes of definite ($\pm$) signature,

$$A^{\pm}(s,t)=\frac{1}{\pi}\int_{t_0}^{\infty}\frac{D_t(s,t')}{t'-t}dt'\pm\frac{1}{\pi}\int_{u_0}^{\infty}\frac{D_u(s,u')}{u'-t}du'$$
$$=\frac{1}{\pi^2}\int^{\infty}\int\frac{\rho_{st}(s'',t')\pm\rho_{su}(s'',t')}{(s''-s)(t'-t)}ds''dt'$$
$$+\frac{1}{\pi^2}\int^{\infty}\int\frac{\rho_{tu}(t',u'')\pm\rho_{tu}(u'',t')}{(u''-u')(t'-t)}du''dt'. \quad (2.2)$$

This is explained in greater detail in, for example, Ref. 1.

The strips are parametrized by the Regge-pole functions of the appropriate channel. Thus the contribution of a given Regge pole to the strip X in the diagram is given by

$$\rho_{st}(s,t)=\Delta_t[\tfrac{1}{2}\pi\Gamma(t)P_{\alpha(t)}(-1-s/2q_t^2)]\theta(s-s_1), \quad (2.3)$$

where

$$\Gamma(t)=[2\alpha(t)+1]\bar{\gamma}(t)(-q_t^2/\hat{t})^{\alpha(t)}, \quad (2.4)$$

$\alpha(t)$ being the trajectory and $\bar{\gamma}(t)\hat{t}^{-\alpha(t)}\equiv\gamma(t)$ the reduced residue. As usual we have taken a factor $\hat{t}^{\alpha(t)}$ out of the reduced residue, so that $\bar{\gamma}(t)$ is of constant dimension for all t. The parameter $\hat{t}$ corresponds to the scale factor in Regge-pole analysis,[1,20] and is chosen so that $\bar{\gamma}(t)$ is a slowly varying function of t.

This piece of double spectral function gives a contribution to the amplitude (see Ref. 10)

$$R^{s_1}(s,t)=\tfrac{1}{2}\Gamma(t)\left\{-\frac{\pi}{\sin\pi\alpha(t)}P_{\alpha(t)}(1+s/2q_t^2)\right.$$
$$\left.-\int_{-4q_t^2}^{s_1}\frac{P_{\alpha(t)}(-1-s'/2q_t^2)}{s'-s}ds'\right\}. \quad (2.5)$$

[20] F. T. Hadjioannou, R. J. N. Phillips, and W. Rarita, Phys. Rev. Letters 9, 183 (1962).

It has been constructed so that it contains the t-channel pole for $\alpha(t)=$integer, has the correct cuts in s, and displays Regge asymptotic behavior

$$\rho_{st}(s,t)\underset{s\to\infty}{\sim}s^{\alpha(t)}. \quad (2.6)$$

The Reggeized Born approximation to the amplitude of isotopic spin I in the s channel consists of putting

$$A^I(s,t)=\sum_i[R_i^{t_1}(s,t)+(-1)^{I_i}R_i^{u_1}(s,u)]\delta_{II_i}$$
$$+\sum_j\beta(I,I_j)[R_j^{s_1}(t,s)+(-1)^{I_j}R_j^{u_1}(t,u)]$$
$$+(-1)^I\sum_k\beta(I,I_k)[R_k^{s_1}(u,s)+(-1)^{I_k}R_k^{t_1}(u,t)], \quad (2.7)$$

the sums being over all the trajectories in the three channels. The $\beta(I,I_j)$, etc., are the π-π isotropic-spin crossing matrices.

The functions $\alpha(t)$ and $\bar{\gamma}(t)$, etc., are arbitrary except for the requirement that they satisfy the usual dispersion relations,[1]

$$\alpha(t)=\alpha(\infty)+\frac{1}{\pi}\int_{t_0}^{\infty}\frac{\mathrm{Im}\alpha(t')}{t'-t}dt' \quad (2.8)$$

and

$$\bar{\gamma}(t)=\frac{1}{\pi}\int_{t_0}^{\infty}\frac{\mathrm{Im}\bar{\gamma}(t')}{t'-t}dt'. \quad (2.9)$$

These forms are required by the Mandelstam representation provided that the trajectories do not cross one another, and provided that our assumptions about the subtractions needed in the dispersions relations are correct. We discuss this further in Sec. V.

To perform a bootstrap it is necessary to relate the s-channel poles to those in the t and u channels by the imposition of unitarity. We try to find values of the Regge parameters which are self-consistent in the sense that the same values are generated in the s channel as are fed into the t and u channels.

The procedure which has been used for imposing unitarity in the new form of the strip approximation is the N/D equations. The strips, with a given choice of input Regge parameters, are used to calculate the left-hand, and far right-hand cuts of the s-channel partial-wave amplitudes, and the corresponding N/D equations are solved.

It was shown in Ref. 10 that the contribution of the t- and u-channel strips to the partial-wave amplitude

is, using the Wong projection,[11]

$$B_l^{sI}(s)=\sum_i \frac{1}{2\pi q_s^{2l+2}}\int_{-\infty}^{0} dt\,\mathrm{Im}\left[Q_l\left(1+\frac{t}{2q_s^2}\right)\right]\left\{\Gamma_j^{II_i}(t)\int_{-4q_t^2}^{s_1} du' P_{\alpha_j(t)}\left(-1-\frac{u'}{2q_t^2}\right)\left[\frac{1}{u'-s}+\frac{(-1)^{I_j}}{u'-u}\right]\right.$$
$$+(-1)^{I_i}\int_{s_1}^{\infty} du'\Gamma_j^{II_i}(t')P_{\alpha_j(t')}\left(-1-\frac{u'}{2q_{t'}^2}\right)\left[\frac{1}{u'-u}-(-1)^I\frac{1}{u'-t}\right]$$
$$\left.+\frac{\pi\Gamma_j^{II_i}(t)}{\sin\pi\alpha_j(t)}\left[(-1)^{I_i}P_{\alpha_j(t)}\left(-1-\frac{s}{2q_t^2}\right)+P_{\alpha(t)}\left(1+\frac{s}{2q_t^2}\right)\right]\right\}, \quad (2.10)$$

where

$$\Gamma_j^{II_i}(t)=\beta(I,I_j)\Gamma_j(t). \quad (2.11)$$

In addition, we can include the s-channel strips, which contribute

$$B_l^{HI}(s)=\sum_j -\frac{1}{4}\int_{-\infty}^{4-t_1} ds'\frac{\Gamma_j(s')\delta_{II_j}}{(s'-s)(-q_{s'}^2)^{l+1}}$$
$$\times\int_{4-s'}^{t_1} dt' P_{\alpha_j(s')}\left(-1-\frac{t'}{2q_{s'}^2}\right)P_l\left(-1-\frac{t'}{2q_{s'}^2}\right) \quad (2.12)$$

to the left-hand cut. Note that we only need to know the Regge parameters for $t<0$ in these formulas. The s-channel trajectory parameters can be obtained from the solution of the N/D equations (see Sec. IV) and the input can be varied until it coincides with the output. This method has the advantage that the N/D equations readily give very accurate values for the output Regge functions, but the disadvantage that only the first Born approximation to the left-hand cut is used. In particular, the "corners" of the double spectral functions (Fig. 1) are not included in the left-hand cut (though the N/D equations calculate them for the right-hand cut automatically). It has been shown that in many circumstances the use of just the first Born approximation to the left-hand cut is not sufficient,[13] and the self-consistent ρ trajectory obtained by this method is a very poor representation of the physical ρ.[9,10]

An alternative method of imposing unitarity is to use the Mandelstam iteration (see Sec. III) to generate the full s-channel strip starting from the t- and u-channel strips.[6–8] Observation of the asymptotic t behavior of the s-channel strips permits the identification of the s-channel Regge poles since

$$D_t^{\pm}(s,t)\xrightarrow[t\to\infty]{}\Gamma(s)\left(\frac{t}{2q_s^2}\right)^{\alpha(s)}\frac{\pi^{1/2}\Gamma(\alpha(s)+\frac{1}{2})}{\Gamma(\alpha(s)+1)}. \quad (2.13)$$

This method has the advantage that it is possible to follow the trajectories even for $s>s_0$. Calculations along these lines have been carried out by Bransden *et al.*[6] and Bali,[8] but only with fixed-spin poles in the t and u channels, not Regge poles. The reason for the relative lack of popularity of this method is that very high numerical accuracy of the iteration routines is needed to isolate the poles. It is also not easy to include other than purely elastic unitarity by this method.

Our procedure is in a sense a combination of these two methods, which we hope will give us the best of both worlds. We calculate the "potential" from the strips as described above, but we also include the contribution of the corners of the double spectral functions to both the left- and right-hand cuts of the partial-wave amplitudes in the N/D equation. These corners are obtained by applying the Mandelstam iteration to the potential, thus unitarizing it.

III. UNITARIZING THE POTENTIAL

The Mandelstam iteration,[14] which was the basis of the old strip approximation of Chew and Frautschi,[15] uses the following equation for the s-channel elastic double spectral function (the region Y in Fig. 1):

$$\rho_{st}^{\mathrm{el}s}(s,t)=\frac{1}{\pi q_s\sqrt{s}}\int_{t_0}^{K=0}\int dt_1 dt_2 \times\frac{D_t^{\pm}(s_+,t_1)D_t^{\pm}(s_-,t_2)}{K^{1/2}(t,t_1,t_2,s)}, \quad (3.1)$$

where

$$K(t,t_1,t_2,s)=[t^2+t_1^2+t_2^2-2(tt_1+tt_2+t_1t_2)-tt_1t_2/q_s^2] \quad (3.2)$$

and s_+, s_- are points above and below (respectively) the s cut of D_t.

The fact that the integration runs only up to $K=0$ means that to calculate $\rho_{st}^{\mathrm{el}s}(s,t)$ out to, say, $t=t_x$ we only need to know $D_t^{\pm}(s,t)$ for $t<t_x$ at a given value of s.

We also have

$$D_t^{\pm}(s,t)=\frac{1}{\pi}\int^{\infty}\frac{\rho_{st}^{\mathrm{el}s}(s'',t)}{s''-s}ds''+D_t^{V\pm}(s,t), \quad (3.3)$$

where $D_t^{V\pm}(s,t)$ is the t discontinuity of the rest of the amplitude other than $\rho_{st}^{\mathrm{el}s}(s'',t)$. In the strip approximation

$$D_t^{V\pm}(s,t)=\Delta_t[2R^{s_1}(s,t)], \quad (3.4)$$

with $R^{s_1}(s,t)$ given by (2.5). We can thus in principle calculate $\rho_{st}^{\mathrm{el}s}(s,t)$ for any s and t given the t- and u-

channel Regge parameters. In fact, as is well known, (3.1) diverges for large s, since if

$$D_t^{\pm}(s,t_1) \underset{s\to\infty}{\sim} s^{\alpha(t_1)} \tag{3.5}$$

for some t_1, we find that after n iterations

$$\rho_{st}^{\mathrm{el}s}(s,t_2) \underset{s\to\infty}{\sim} s^{2\alpha(t_1)-n}, \tag{3.6}$$

for some $t_2>t_1$ (the value of t_2 can be found from t_1 and n using the properties of K).

This divergence (which is connected with the problem of the spurious Amati-Fubini-Stanghellini cuts[21]) is due to the false assumption of elastic unitivity for all s. The difficulty can be circumvented if we rewrite (3.1) as[7]

$$\rho_{st}^{\mathrm{el}s}(s,t)=\frac{g(s)}{\pi q_s\sqrt{s}}\int_{t_0}^{K=0}\int dt_1dt_2 \times\frac{D_t^{\pm}(s_+,t_1)D_t^{\pm}(s_-,t_2)}{K^{1/2}(t,t_1,t_2,s)}, \tag{3.7}$$

where $g(s)$ is some cut-off function. In our calculation we have followed Bali[8] in using

$$g(s)=\{1+\exp[(s-s_1)/\Delta]\}^{-1}. \tag{3.8}$$

With this cutoff we can calculate $\rho_{st}^{\mathrm{el}s}(s,t)$ out to $s=s_1$ without there being any singularity of $\rho_{st}^{\mathrm{el}s}(s,t)$ at the boundary, as would be the case if we simply terminated the integration of (3.1) at $s=s_1$. Above s_1 we expect the double spectral function to be given by the t-channel strip (see Fig. 1).

We could, as mentioned in the previous section, use (3.7) to generate $\rho_{st}^{\mathrm{el}s}(s,t)$ for high values of t, and attempt to find the s-channel Regge trajectories from the asymptotic behavior. However, the strip approximation already includes the asymptotic part of the double spectral function so we are only concerned with using (3.7) to calculate $\rho_{st}^{\mathrm{el}s}(s,t)$ for $t<t_1$. In practice we shall always use $s_1=t_1$ as in Fig. 1. Obviously, (3.4) demands a knowledge of the Regge parameters for $t>0$, unlike (2.10) and (2.12).

Crossing symmetry requires that the other corner regions of the double spectral functions shown in the diagram (Fig. 1) should be the same as $\rho_{st}^{\mathrm{el}s}(s,t)$ apart from permutation of the variables. More precisely,

$$\begin{aligned}\rho_{st}^{\mathrm{el}t}(s,t)&=\rho_{st}^{\mathrm{el}s}(t,s),\\ \rho_{tu}^{\mathrm{el}t}(t,u)&=\rho_{st}^{\mathrm{el}s}(t,u),\\ \rho_{tu}^{\mathrm{el}u}(t,u)&=\rho_{st}^{\mathrm{el}s}(u,t).\end{aligned} \tag{3.9}$$

As a digression we may note that at this stage one could use these results in (2.2) to obtain new values of $D_t^V(s,t)$ which could be used in (3.1) to find a new value of $\rho_{st}^{\mathrm{el}s}(s,t)$. Repeating this cycle a few times would give a more self-consistent $\rho_{st}^{\mathrm{el}s}(s,t)$. In practice, we have not found that this makes much difference in the values of $\rho_{st}^{\mathrm{el}s}(s,t)$ that are obtained. In any case the existence of $\rho_{st}^{\mathrm{el}t}(s,t)$ implies that it is not strictly correct to use elastic unitarity for $s>s_I$ (s_I being the inelastic threshold in the s channel; $=16m_\pi^2$ for π-π scattering). The advantage of going to this extra trouble is thus doubtful, and in this paper we assume that the elastic double spectral functions calculated as above are a sufficiently good approximation for obtaining the left-hand cut of the N/D equations. But we shall include this inelasticity in the right-hand cut (see Sec. IV).

The contribution of these double spectral functions to the full amplitude is of course obtained by substituting them in (2.2), i.e.,

$$A^{\pm}(s,t)=\frac{1}{\pi^2}\int^{s_1}\int\frac{\rho_{st}^{\mathrm{el}t}(s'',t')\pm\rho_{su}^{\mathrm{el}u}(s'',t')}{(s''-s)(t'-t)}ds''dt' +\frac{1}{\pi^2}\int^{s_1}\int\frac{\rho_{tu}^{\mathrm{el}t}(t',u'')\pm\rho_{tu}^{\mathrm{el}u}(u',t')}{(u''-u')(t'-t)}du''dt'. \tag{3.10}$$

Our complete approximation to the scattering amplitude is the sum of (3.10) and the six strip contributions (2.7).

IV. N/D EQUATIONS

As in the previous calculations[9,10] we shall use the N/D equations to impose unitarity on the partial-wave amplitudes of definite signature. The "reduced" partial-wave amplitude is given by the Froissart-Gribov projection,[22]

$$B_l^{\pm}(s)\equiv A_l^{\pm}(s)q_s^{-2l} =\frac{1}{2\pi}\int_{t_0}^{\infty}D_t^{\pm}(s,t)Q_l\left(1+\frac{t}{2q_s^2}\right)\frac{dt}{q_s^{2l+2}}, \tag{4.1}$$

and we write it in the form

$$B_l^{\pm}(s)=[\eta_l(s)e^{2i\delta_l(s)}-1]/2i\rho_l(s), \tag{4.2}$$

with

$$\rho_l(s)=\left(\frac{s-4m_\pi^2}{s}\right)^{1/2}\left(\frac{s-4m_\pi^2}{4}\right)^{l}. \tag{4.3}$$

The phase shift has been decomposed into its real and imaginary parts (for real s),

$$\delta_l(s)=\delta_l^R(s)+i\delta_l^I(s) \tag{4.4}$$

and

$$\eta_l(s)\equiv e^{-2\delta_l^I(s)}. \tag{4.5}$$

[21] D. Amati, S. Fubini, and A. Stanghellini, Phys. Letters 1, 29 (1962).

[22] M. Froissart, invited paper at the La Jolla Conference on Weak and Strong Interactions, 1961 (unpublished); V. N. Gribov, Zh. Eksperim. i Teor. Fiz. 41, 667 (1961) [English transl.: Soviet Phys.—JETP 14, 478 (1962)].

The function $\eta_l(s)$ gives the inelasticity, and

$$\eta_l(s)=1 \quad \text{for} \quad s_0<s<S_I, \tag{4.6}$$

$$0<\eta_l(s)<1 \quad \text{for} \quad s>s_I. \tag{4.7}$$

We follow the method of Frye and Warnock[16] (see also Ref. 1) in factoring the amplitudes into

$$B_l(s)=N_l(s)/D_l(s) \tag{4.8}$$

and giving $D_l(s)$ a right-hand cut for $s_0<s<s_1$ with phase $e^{-i\delta l^R(s)}$. All the other cuts of $B_l(s)$ are put into $N_l(s)$. From (4.2)

$$N_l(s)=B_l(s)D_l(s)=[\eta_l(s)D_l{}^*(s)-D_l(s)]/2i\rho_l(s), \tag{4.9}$$

and taking the real and imaginary parts we get

$$\mathrm{Im}\{N_l(s)\}=\frac{1-\eta_l(s)}{2\rho_l(s)}\mathrm{Re}\{D_l(s)\}, \quad s_I<s<s_1 \tag{4.10}$$

$$\mathrm{Im}\{D_l(s)\}=\frac{-2\rho_l(s)}{1+\eta_l(s)}\mathrm{Re}\{N_l(s)\}, \quad s_0<s<s_1. \tag{4.11}$$

We define the potential function

$$B_l{}^V(s)\equiv\int_{-\infty}^{s_L}\frac{\mathrm{Im}B_l(s')}{s'-s}ds'+\int_{s_1}^{\infty}\frac{\mathrm{Im}B_l(s')}{s'-s}ds' \tag{4.12}$$

and

$$\bar{B}_l{}^V(s)\equiv B_l{}^V(s)+\frac{P}{\pi}\int_{s_I}^{s_1}\frac{1-\eta_l(s')}{2\rho_l(s')}\frac{ds'}{(s'-s)}, \tag{4.13}$$

and also define

$$\bar{N}_l(s)\equiv\frac{2\eta_l(s)}{1+\eta_l(s)}\mathrm{Re}\{N_l(s)\}. \tag{4.14}$$

Then, writing dispersion relations for $D_l(s)$ and $\{N_l(s)-B_l{}^V(s)D_l(s)\}$, we end up with the Frye-Warnock form of the N/D equations modified for the strip approximation, viz.,

$$\bar{N}_l(s)=\bar{B}_l{}^V(s)+\frac{1}{\pi}\int_{s_0}^{s_1}\frac{\bar{B}_l{}^V(s')-\bar{B}_l{}^V(s)}{s'-s}\times\frac{\rho_l(s')\bar{N}_l(s')}{\eta_l(s')}ds', \tag{4.15}$$

$$D_l(s)=1-\frac{1}{\pi}\int_{s_0}^{s_1}\frac{\rho_l(s')\bar{N}_l(s')}{\eta_l(s')(s'-s)}ds'. \tag{4.16}$$

Hence we can find $B_l(s)$ from the unitarity condition (4.2) given $B_l{}^V(s)$ and $\eta_l(s)$ as input.

If we divide $\mathrm{Im}\{B_l(s)\}$ for $S_I<s<s_1$ into its elastic and inelastic parts,[7]

$$\mathrm{Im}\{B_l(s)\}=\rho_l(s)|B_l(s)|^2+\mathrm{Im}\{B_l{}^I(s)\}, \tag{4.17}$$

and substitute these expressions in (4.2), we find

$$\eta_l(s)=[1-4\rho_l(s)\ \mathrm{Im}\{B_l{}^I(s)\}]^{1/2}. \tag{4.18}$$

Now $B_l{}^V(s)$ is the sum of (2.10), (2.12), and the contributions of the corners of the double spectral functions (3.10) to the left-hand cut of $B_l(s)$ [$\equiv B_l{}^{\mathrm{Lc}}(s)$, say]. The latter may be obtained by substituting (3.9) in (2.2), and then in (4.1), giving (say)

$$B_l{}^c(s)=\frac{1}{2\pi}\int^{s_1}\int\left[\frac{\rho_{st}(s'',t')\pm\rho_{su}(s'',t')}{s''-s}ds''+\frac{\rho_{tu}(t',u'')\pm\rho_{tu}(u',t')}{u''-u'}du''\right]Q_l\left(1+\frac{t'}{2q_s{}^2}\right)\frac{dt'}{q_s{}^{2l+2}}. \tag{4.19a}$$

The first term of (4.19a) contributes also to the right-hand cut of $B_l(s)$, and if we remove this right-hand-cut part (see Ref. 23) we end up with

$$B_l{}^{\mathrm{Lc}}(s)=\frac{1}{2\pi}\int^{s_1}\int\left[\frac{\rho_{st}(s'',t')\pm\rho_{su}(s'',t')}{s'-s}\right]\times\left[\frac{Q_l(1+t'/2q_s{}^2)}{q_s{}^{2l+2}}-\frac{Q_l(1+t'/2q_s{}''^2)}{q_s{}''^{2l+2}}\right]ds''dt'+\frac{1}{2\pi}\int^{s_1}\int\left[\frac{\rho_{tu}(t',u'')\pm\rho_{tu}(u'',t')}{u''-u'}\right]\times\frac{Q_l(1+t'/2q_s{}^2)}{q_s{}^{2l+2}}du''dt'. \tag{4.19b}$$

The contribution of $\rho_{st}{}^{\mathrm{el}t}(s,t)$ to $\mathrm{Im}\{B_l(s)\}$ is

$$\mathrm{Im}\{B_l{}^I(s)\}=\int^{s_1}[\rho_{st}{}^{\mathrm{el}t}(s,t')\pm\rho_{su}{}^{\mathrm{el}u}(s,t')]\times\frac{Q_l(1+t'/2q_s{}^2)}{2q_s2^{l+2}}dt'. \tag{4.20}$$

Hence, within the approximations of Sec. III, we have $\eta_l(s)$ given by (4.18) and (4.20), and [see (2.10) and (2.12)]

$$B_l{}^V(s)=B_l{}^{sI}(s)+B_l{}^{HI}(s)+B_l{}^{\mathrm{Lc}}(s), \tag{4.21}$$

and the N/D equations can be solved with the input of Sec. II.

As usual the output, s-channel, Regge-trajectory parameters can be obtained from

$$D_{\alpha(s)}(s)=0 \tag{4.22}$$

and

$$\gamma(s)/\alpha'(s)=[N_l(s)/D_l{}'(s)]|_{l=\alpha(s)} \tag{4.23}$$

(the prime indicates d/ds). Our bootstrap procedure thus consists of putting t- and u-channel trajectory parameters into (2.3), finding the corresponding potential (4.21), and $\eta_l(s)$ (4.18) solving the N/D equations, and thus finding the output s-channel parameters. We adjust the input until it coincides with the output.

[23] P. D. B. Collins, Phys. Rev. 139, B696 (1965).

V. ρ BOOTSTRAP

As an example of the above procedure we have attempted to bootstrap the ρ in π-π scattering. It has been shown that the force from the exchange of a ρ trajectory will also generate an $I=0$ Pomeranchon trajectory.[9,10] The inclusion of this trajectory calls for special treatment which we hope to discuss in a further paper, and we shall restrict ourselves to a discussion of ρ exchange alone. This approximation has been discussed by many authors,[2-5] and has been tried both in the new strip approximation[9] and in the Mandelstam iteration method.[8]

We parametrize the input trajectory function by[24]

$$\mathrm{Im}\alpha(t)=\frac{c_1 x^\lambda}{(x-a_1)^2+b_1^2}, \quad x\equiv t-4m_\pi^2 \tag{5.1}$$

which, substituted in (2.8), gives

$$\alpha(t)=\alpha(\infty)+\frac{c_1\csc(-\pi\lambda)}{(x-a_1)^2+b_1^2}\left\{(e^{-i\pi}x)^\lambda + \frac{(a_1^2+b_1^2)^{\lambda/2}}{b_1}[(x-a_1)\sin\lambda\phi_1+b_1\cos\lambda p_1]\right\}, \tag{5.2}$$

and the residue by

$$\mathrm{Im}\bar{\gamma}(t)=c_2 x^\lambda(x-d)/[(x-a_2)^2+b_2^2], \tag{5.3}$$

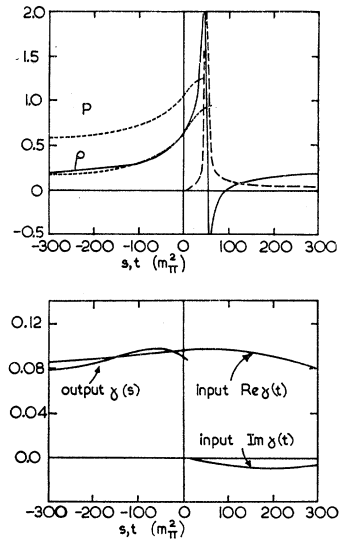

FIG. 2. Self-consistent ρ trajectory, and residue, functions (input $\mathrm{Re}\alpha_P\equiv$———, input $\mathrm{Im}\alpha_P\equiv$— — —, output $\mathrm{Re}\alpha_P$ and $\mathrm{Re}\alpha_P$=– – – –). The parameters (see text) are $s_1=1000$, $\Delta=50$, $\bar{t}=200$, $a_1=47.0$, $b_1=3.94$, $c_1=1.05$, $a_2=540.0$, $b_2=392.5$, $c_2=0.068$, and $d=420$, all in m_π^2 units. This corresponds to an input ρ width $\Gamma_{\mathrm{in}}=147$ MeV, but the output width $\Gamma_{\mathrm{out}}=340$ MeV.

[24] A. Ahmadzadeh and I. A. Sakmar, Phys. Letters **5**, 145 (1963).

which in (2.9) gives

$$\bar{\gamma}(t)=\frac{c_2\csc(-\pi\lambda)}{(x-a_2)^2+b_2^2}\left[(e^{-i\pi}x)^\lambda(x-d)+\frac{(a_2^2+b_2^2)^{\lambda/2}}{b_2} \times\{[(d-a_2)(x-a_2)+b_2^2]\sin\lambda\phi_2-b_2(x-a_2)\cos\lambda\phi_2\}\right]$$

where

$$\phi_i=\tan^{-1}(b_i/a_i)-\pi, \quad i=1,2. \tag{5.4}$$

The form of these functions is shown in Fig. 2.

Note that $\mathrm{Im}\alpha$ must be positive by unitarity, but there is no such restriction on $\mathrm{Im}\bar{\gamma}$. Both $\mathrm{Im}\alpha$ and $\mathrm{Im}\bar{\gamma}$ must vanish at the threshold, and we are assuming that the integrals (2.8) and (2.9) can be written without subtractions, so that

$$\mathrm{Im}\bar{\gamma}(t), \quad \mathrm{Im}\alpha(t)<O(t^{-1}). \tag{5.5}$$

We are also assuming that

$$\alpha(s)\underset{s\to\infty}{\longrightarrow}\text{const} \tag{5.6}$$

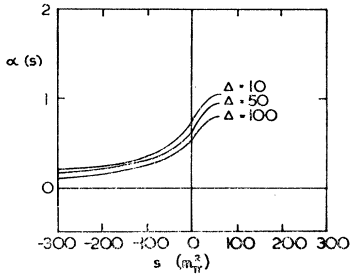

FIG. 3. The output ρ trajectories which result with the indicated values of Δ. All the other parameters are as in Fig. 2.

as it does in potential scattering. If $\alpha(s)\to\pm\infty$ we cannot expect our single-channel bootstrap to work, though it may still give a reasonable approximation to the trajectory over a limited region of s near $s=0$ (see Refs. 17 and 18 for a discussion of this). The input width of the ρ meson corresponding to these functions is given by

$$\Gamma_{\mathrm{in}}=\frac{\mathrm{Im}\{\alpha(m_\rho^2)\}}{m_\rho\,\mathrm{Re}\{\alpha'(m_\rho^2)\}}\approx\frac{\mathrm{Re}\{\gamma(m_\rho^2)\}}{m_\rho\,\mathrm{Re}\{\alpha'(m_\rho^2)\}}\rho_l(m_\rho^2). \tag{5.7}$$

These parameters are used in (2.3) and (3.4) to find $\rho_{st}^{\mathrm{el}s}(s\,t)$ for a given value of $s_1=t_1$ and Δ. It is evident that the number of iterations which we need to find $\rho_{st}^{\mathrm{el}s}(s\,t)$ depends on how large is t_1. The main weight of D_t^V at the point where $\mathrm{Im}\alpha$ is a maximum, and since this must be above the ρ mass (since the trajectory is rising through the position of the ρ meson) the number of iterations needed for, say, $s_1=2000\,m_\pi^2$ is only 6 or 7. The calculated double spectral function is then used in (4.19) to find $B_l^{\mathrm{Lc}}(s)$ and to find $\eta_l(s)$.

There are thus 11 input parameters, a_1, b_1, c_1, $\alpha(\infty)$, d, a_2, b_2, c_2, $\bar{t}$, s_1, and Δ. The first nine of these are to be

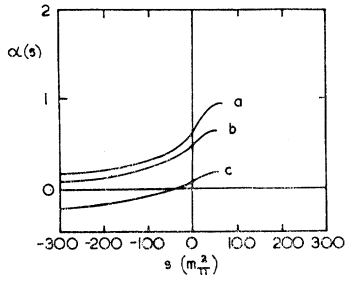

FIG. 4. (a) The self-consistent ρ trajectory of Fig. 2; (b) the output trajectory obtained when η is set equal to 1; and (c) that obtained when only the strip contributions are included in the left-hand cut, i.e., the first Born approximation.

made consistent with the output, so there are just two free parameters, the cutoff's s_1 and Δ. Our bootstrap is only really self-consistent if the dependence on the choice of s_1 and Δ is small. Since Δ only determines the "width" of $g(s)$ in (3.8) the results are in fact only trivially dependent on it, as Fig. 3 demonstrates. In all the rest of the results quoted in this paper it is fixed at $\Delta=50$. Also the scale factor in the residue function $\tilde{t}$, which we expect to be roughly $\frac{1}{2}s_1$,[25] has been fixed at $200m_\pi^2$ throughout.

A self-consistent ρ trajectory is shown in Fig. 4. It has been chosen so that its parameters correspond to the physical meson by having $\alpha(30)=1$, and the experimental input width $\Gamma_{\text{in}}=147$ MeV.[26] The output width is still much too large, however, $\Gamma_{\text{out}}=340$ MeV. The trajectory is not qualitatively different from those obtained in previous work,[9,10] where the second and higher Born approximations to the potential were not included, but a good deal of extra force has been obtained.

Part of this extra force is due to the inclusion of inelasticity, and also show the trajectory which is obtained with $\eta_l(s)=1$ rather than the calculated value. The variation of $\eta_l(s)$ with s for various values of l is shown in Fig. 5. The corresponding values at s_1 [calculated by substituting $\text{Im}\{B_l^V(s_1)\}$ from the strip region in (4.18)] are also indicated in the figure. They do not match on completely, of course, since nothing has been done to make them consistent, but the discrepancy is not too bad, except that for $l<0.2$ unitarity is violated above s_1. This problem has been noted previously,[10] and is due to the fact that the self-consistent results tend to have too

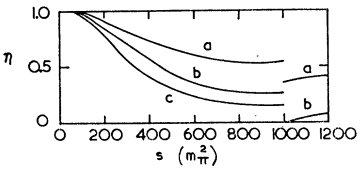

FIG. 5. A plot of the inelasticity $\eta_l(s)$ against s with the parameters of Fig. 2, for (a) $l=1.0$, (b) $l=0.2$, and (c) $l=0.0$. The values calculated from the strips above s_1 ($=1000$) are also shown, and we see that for $l<0.2$ unitarity is violated at s_1.

[25] G. F. Chew and V. L. Teplitz, Phys. Rev. **136**, B1154 (1964).
[26] J. Pisut and M. Roos, Nucl. Phys. **B6**, 325 (1968).

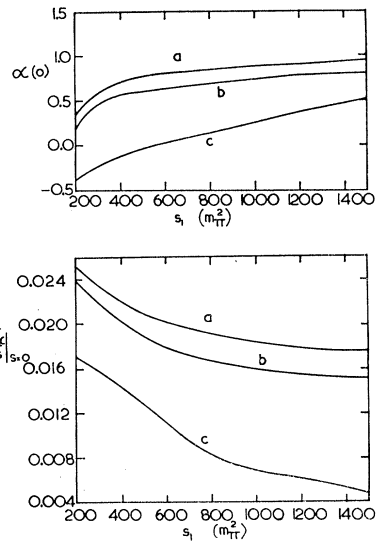

FIG. 6. Plots of $\alpha(0)$ and $\alpha'(0)$ against s_1 with all the other parameters fixed. The three cases are (a) the complete calculation, (b) η set equal to 1, and (c) only the strip contributions included in left-hand cut. The dependence on the choice of s_1 is much reduced by including the elastic double spectral function.

large a value of $\gamma(t)$ for $t<0$. This is compensated by having a large $\alpha'(s)$ in the region of the ρ meson by putting the peak of $\text{Im}\alpha(s)$ not far above the mass of the particle (see Fig. 2). The problem[10] of needing a large input width to generate enough force to produce a reasonable output trajectory is thus circumvented.

The dependence of the results on the choice of s_1 is shown in Fig. 6. We see that the position of $\alpha(0)$ is little affected by the value of this parameter provided we take $s_1\gtrsim 800m_\pi^2$, and is much reduced by the inclusion of higher Born approximations. The slope tends to decrease with increasing s_1, but again the higher Born approximations make the results almost independent of this arbitrary parameter if it is sufficiently large. The dependence is certainly not so great as to make one feel that it is playing a dominant role.

In Fig. 7 we show the variations of $\rho_{st}^{\text{els}}(s,t)$ with t for some values of s. The first peak corresponds to the first iteration of those in $D_l(s,t)$ due to the particle at $t=m_\rho^2$ and the maximum of $\text{Im}\alpha(t)$ just above it, and

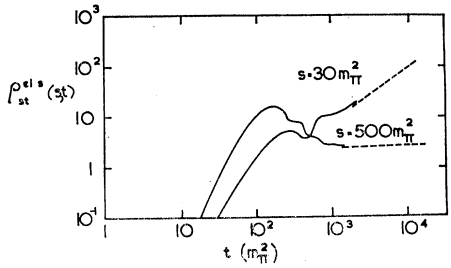

FIG. 7. A plot of $\rho_{st}^{\text{els}}(s,t)$ against t for two values of s. The dashed line is the asymptotic strip for $t<s_1$, and matches rather well, showing that we have indeed reached the asymptotic region for $t\gtrsim 1000m_\pi^2$.

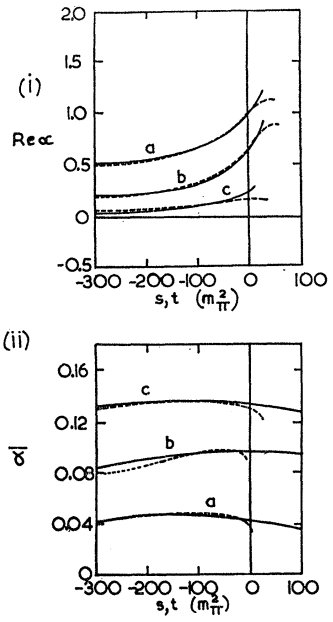

FIG. 8. Self-consistent ρ (i) trajectories, and (ii) residues, with (a) $\alpha(0)=1.0$, $\alpha(\infty)=0.49$; (b) $\alpha(0)=0.57$, $\alpha(\infty)=0.17$; and (c) $\alpha(0)=0.17$, $\alpha(\infty)=0.03$. The dashed lines are the output, and the full lines the input Regge functions. Once $\alpha(\infty)$ has been decided upon, the demand for self-consistency fixes the shape of the trajectory. The width of the $l=1$ resonances in the three cases are (a) bound state, (b) 350 MeV, (c) 630 MeV. Note that case (b) is similar to, but slightly different from, Fig. 2. The parameters which have been changed are $b_2=400$ and $c_2=0.76$. This indicates the amount of variation which can be tolerated in these parameters.

the subsequent maxima are due to the further iterations. The double spectral function has settled down to its asymptotic value for $t\approx 1000m_\pi^2$, and so we take this as our preferred value of s_1. The double spectral function calculated in this way matches smoothly onto the asymptotic strip region above s_1.

The chief problem in this type of calculation lies in determining the range of parameters over which "reasonable" self-consistency can be obtained We have found that at the unitarity limit, $\alpha(0)=1$, it is possible to obtain such a solution and, for lower values down to $\alpha(0)\approx 0.2$. Some examples are shown in Fig. 8.

It will be noted that the basic shape of the residue function is always the same. It agrees with the Chew-Teplitz form,

$$\bar{\gamma}(t)=\text{const}\,\alpha'(t)(\bar{t}-t)Q_{\alpha(t)}\left(1+\frac{2m_\rho^2}{\bar{t}-4m_\pi^2}\right), \quad (5.8)$$

which was deduced in Ref. 26 from the form of the N/D equations. The only way of avoiding this shape is for there to be changes of sign of $B_l^V(s)$ in the strip region. The need for such oscillations, if we are to find residues with a rapid decrease for negative t, like those found in many fits to the experimental data, has been discussed in Ref. 27. With only the attractive ρ-exchange potential we cannot expect oscillations, though we can hope that they will occur when the Pomeranchon repulsion is included. The form of $\mathrm{Im}\bar{\gamma}(t)$ in (5.3) has been chosen to reproduce (5.8) for negative t, and the change of sign at $t=d+4m_\pi^2$ seems to be the easiest way of achieving this.

Since the output shape of $\bar{\gamma}(s)$ is always much the same, the values of d, a_2, and b_2 are more or less fixed. The value of λ should correspond to the known threshold behavior[1] of $\mathrm{Im}\bar{\gamma}(t)$, which is

$$\mathrm{Im}\bar{\gamma}(t)\underset{t\to t_0}{\sim}(t-t_0)^{\alpha(t_0)+1/2}.$$

In practice we have fixed $\lambda=0.5$ for all $\alpha(0)$. This has been found to make rather little difference so long as λ does not approach too close to 1, when the integral (2.9) would diverge. The only really free parameter, which is not determined by the shape of the output residue, is the over-all magnitude c_2. It is this which is determined by demanding self-consistency of input and output, and ranges from $c_2=0.093$ for $\alpha(0)=1$ to $c_2=0.028$ for $\alpha(0)=0.2$.

Similarly, the range of shapes of the output trajectories exhibited in solutions shown in Fig. 8 is very limited, and the only really significant free parameter in (5.2) is the absolute height of the trajectory determined by $\alpha(\infty)$. Again λ was fixed at 0.5, though in this case the integral (2.8) converges for $\lambda<2$. The values of a_1, b_1, and c_1 are essentially fixed by the form of the output. As far as we have been able to discover the trajectories shown in Fig. 8 span the full range of parameters for which reasonable self-consistency can be achieved. It has not proved possible to get a self-consistent trajectory with $\alpha(\infty)<0$ for any choice of input parameters. Such trajectories produced much too little force. To get a trajectory like the experimental ρ (for example, in Ref. 28) we would like a much smaller curvature, but Fig. 8 shows that the amount of curvature is always about the same.

It will be noted from Fig. 5 that, as in earlier calculations,[10] though the input and output trajectories agree very closely for $t<0$ it is not possible to make them agree for $t\gg 0$, and in fact $\mathrm{Re}\{D_l(s)\}$ for $l\gtrsim 0.9$ does not have a zero in the solution shown in Fig. 8. The output widths quoted in Figs. 4 and 8 were obtained by plotting out the partial-wave cross section. They are something of an improvement over earlier calculations, but the problem of achieving a sufficiently narrow ρ has certainly not been solved.

There is a related difficulty that, because of the bunching of $\mathrm{Im}\alpha(t)$ in a peak just above the ρ mass, $D_t^{V\pm}(s,t)$ calculated from (3.4) also has a peak there, and has the sort of shape plotted in Fig. 9. Normally one would expect the maximum of $D_t^{V\pm}(s,t)$ to be at

[27] P. D. B. Collins, Phys. Rev. **157**, 1432 (1967).

[28] G. Hohler, H. Schaile, and P. Sonderegger, Phys. Letters **20**, 79 (1966).

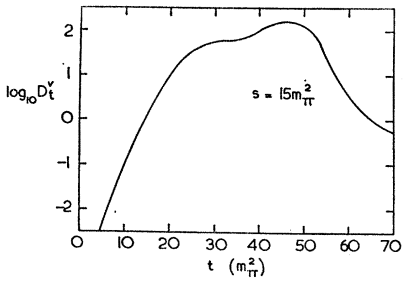

FIG. 9. A plot of $\log_{10} D_t{}^{l=1}(s,t)$ against t for $s=15\ m_\pi{}^2$. It shows the first peak of D_t due to the particle at $t=30\ m_\pi{}^2$ and the second and larger peak due to that of Imα at $t=47\ m_\pi{}^2$.

$t=m_\rho{}^2$ (there is a secondary peak there) corresponding to to the vanishing of $\sin\pi\alpha(t)$.

A large Im$\alpha(t)$ of this sort is essential in our parametrization if we are to obtain a trajectory with a curvature like that of the output. This peak of $D_t{}^{V\pm}(s,t)$ implies that there is a peak of the t-channel cross section, but no such peak is evident in our output c-channel cross sections. Full crossing symmetry has thus not been achieved. In Bali's calculations[8] (see Fig. 8 of his paper) Im$\alpha(t)$ was a continuously increasing function right up to the boundary of the strip, $t=s_1$, and an iteration of such an input would not settle down to its asymptotic form unitl $t\gg s_1$. One can hope to improve the satisfaction of crossing symmetry by choosing one's parameters to ensure that the t- and s-channel partial-wave cross sections are consistent, but it is probably not worth worrying about this until the Pomeranchon has been included as well.

VI. CONCLUSIONS

We have succeeded in bootstrapping a ρ trajectory with the physical mass, width, and intercept $\alpha(0)$. This is one of a range of rather similar self-consistent solutions with $\alpha(0)$ ranging from the unitarity bound of 1 down to about 0.2. The physical trajectory is thus not uniquely predicted in our approximation.

Also the output trajectory is only known to be similar to the input in the region $t<0$. For $t\gg0$ is not possible to trace the output trajectory, and we can not be certain that it goes through $l=1$ on the unphysical sheet. This was also the case in the new strip approximation,[10] but not in the iterative calculation of Bali.[8] No calculation has ever been able to obtain trajectories which rise much above $l=2$ and if the physical trajectories do this we cannot hope to reproduce them in a single-channel calculation of this type.

Similarly since there are no superconvergence relations built into our potential we know that the endpoint of the trajectory, $\alpha(\infty)$, must be at some dynamically determined point above $l=-1$.[12] Unfortunately it seems to be impossible to get an output trajectory which does not have considerable curvature, and so ends up above $l=0$. Because $\alpha(s)$ is a Herglotz function, this curvature means that Im$\alpha(s)$ must have its maximum not far above threshold, and this makes the trajectory turn over rather soon on the right-hand cut. We have discussed elsewhere[17] the implications of straight Regge trajectories with narrow resonances for bootstrap calculations and will not repeat the arguments further here. We can still hope that the single-channel calculations will give a worthwhile approximation to the trajectories in the region near $t=0$.

It is probably worth reminding the reader that, because the Wong projection is used in (2.10), the strip contribution to the potential depends only on the Regge parameters for $t<0$, where complete self-consistency has been obtained. The corners of the double spectral functions depend on the Regge parameters for $t>t_0$, and it is not possible to continue the solutions onto the unphysical sheet to find the zeros of $D_l(s)$. Despite the fact that our parametrization of Im$\alpha(t)$ fits the output $\alpha(t)$ for $t<0$ through the dispersion relation, the correspondence is probably not very good above threshold, because the sharp peak of Im$\alpha(t)$ in the input does not seem to be reproduced in the output. There is very little freedom in the possible form of the output trajectory for $t<0$, and only its height $\alpha(\infty)$ is variable to any significant extent.

Very similar remarks apply to the residue function which is almost constant, and, in order to produce a self-consistent trajectory, has to be very large (though smaller than is required if we do not iterate the potential). This size results in a violation of unitarity for low values of l. The magnitude of the residue does not mean that the input ρ meson is too wide, however, because the trajectory is very strongly curved and has a large slope at the position of the meson. But the output ρ is certainly too wide by a factor of 2.

There is still hope that some of these deficiencies will be rectified when the Pomeranchon is included as a force, and we hope to return to this in a further publication, but it seems all too likely that even then we shall not be able to obtain a trajectory which is similar to the physical ρ.

Calculations of the type described in this paper probably represent the maximum of sophistication which is worthwhile within the confines of a single channel, and if there is to be further progress it will probably be necessary to perform multichannel calculations, including particles with high spin. The approximate multichannel calculations which have been attempted so far[4,5,29] have not produced results sufficiently different from the single-channel ones to make one feel optimistic about this, however. We do not really know any way round the fundamental difficulties of the bootstrap philosophy described in Ref. 17.

[29] N. F. Bali and S.-Y. Chiu, Phys. Rev. 153, 1579 (1967).